Clifford I. Voss* and George F. Pinder**

1.0 Introduction

The simulation of geothermal reservoirs involves the solution of the equations describing multiphase, non-isothermal flow in porous media. These equations are highly nonlinear, particularly as the solution encounters the boundary of the two-phase region. There are essentially as many ways of accommodating this nonlinearity as there are numerical models of geothermal reservoirs. However, there is no universally accepted method for establishing the relative accuracy of these techniques. Well-established methodologies such as Fourier analysis and comparison against analytical solutions are simply not applicable to nonlinear systems. A necessary but not sufficient condition for convergence is the conservation of mass energy and momentum. This information is generally provided as an integral part of the numerical solution.

2.0 Governing Equations

One possible form of the equations governing mass and energy transport in geothermal reservoirs is:

$$\Bigg[(1-\theta)\rho_m\left(\frac{\partial h_m}{\partial p_f}\right)_{h_f} - \theta\Bigg]\frac{\partial p_f}{\partial t} + \Bigg[(1-\theta)\rho_m\left(\frac{\partial h_m}{\partial h_f}\right)_{p_f} + \theta\rho_f\Bigg]\frac{\partial h_f}{\partial t} - \Bigg[\left(\frac{\underset{\approx}{k}k_{rs}\rho_s}{\mu_s} + \frac{\underset{\approx}{k}k_{rw}\rho_w}{\mu_w}\right)$$

$$\cdot\, \underset{\sim}{\nabla} p_f - \left(\frac{\underset{\approx}{k}k_{rs}\rho_s^2}{\mu_s} + \frac{\underset{\approx}{k}k_{rw}\rho_w^2}{\mu_w}\right)\cdot \underset{\sim}{g}\Bigg]\cdot \underset{\sim}{\nabla} h_f + \underset{\sim}{\nabla}\cdot\Bigg\{\Bigg[\left(\frac{1}{\rho_f}\right) S_s S_w \rho_s \rho_w (h_s - h_w)$$

$$\cdot\left(\frac{\underset{\approx}{k}k_{rw}}{S_w\mu_w} - \frac{\underset{\approx}{k}k_{rs}}{S_s\mu_s}\right) - \kappa\left(\frac{\partial T}{\partial p_f}\right)_{h_f}\underset{\approx}{I}\;\Bigg]\cdot \underset{\sim}{\nabla} p_f\Bigg\} - \underset{\sim}{\nabla}\cdot\left(\kappa\frac{\partial T}{\partial h_f}\underset{\sim}{\nabla} h_f\right) - \underset{\sim}{\nabla}\cdot \qquad (1)$$

$$\Bigg\{\left(\frac{1}{\rho}\right) S_s S_w \rho_s \rho_w (h_s - h_w)\Bigg[\left(\frac{\underset{\approx}{k}k_{rw}\rho_w}{S_w\mu_w} - \frac{\underset{\approx}{k}k_{rs}\rho_s}{S_s\mu_s}\right)\cdot \underset{\sim}{g}\Bigg]\Bigg\} - \varepsilon\rho_f(\underset{\sim}{V}_f\cdot \underset{\sim}{g}) = 0 \qquad \text{energy}$$

$$\theta\left(\frac{\partial\rho_f}{\partial p_f}\right)_{h_f}\frac{\partial p_f}{\partial t} + \theta\left(\frac{\partial\rho_f}{\partial h_f}\right)\frac{\partial h_f}{\partial t} - \underset{\sim}{\nabla}\cdot\Bigg[\left(\frac{\underset{\approx}{k}k_r\,\rho_s}{\mu_s} + \frac{\underset{\approx}{k}k_r\,\rho_w}{\mu_w}\right)\cdot \underset{\sim}{\nabla} p_f \qquad (2)$$

$$-\underset{\sim}{\nabla}\cdot\Bigg[\left(\frac{\underset{\approx}{k}k_{rs}\rho_s^2}{\mu_s} + \frac{\underset{\approx}{k}k_{rw}\rho_w^2}{\mu_w}\right)\cdot \underset{\sim}{g}\Bigg] = 0 \qquad \text{(mass)}$$

---

*Dept. of Water Resources Eng., The Royal Institute of Technology, S-100 44, Stockholm 70, Sweden.

**Dept. of Civil Engineering, Princeton University, Princeton, N.J.

3.0 Nonlinear Coefficients

These equations are formulated in terms of two dependent variables, h_f and p_f. The remaining thermodynamic properties, e.g., ρ_s, ρ_w, are expressed in terms of h_f and p_f through highly nonlinear relationships. The degree of nonlinearity is apparent in Fig. 1, where a few of the nonlinear coefficients are presented:

$$C_1 \equiv \left(\frac{\underset{\approx}{k} k_{rs} \rho_s}{\mu_s} + \frac{\underset{\approx}{k} k_{rw} \rho_w}{\mu_w} \right)$$

$$C_2 \equiv \theta \left(\frac{\partial \rho_f}{\partial p_f} \right)_{h_f}$$

$$C_3 \equiv \theta \left(\frac{\partial \rho_f}{\partial h_f} \right)_{p_f}$$

$$C_4 \equiv \kappa \left(\frac{\partial T}{\partial p_f} \right)_{h_f} + \frac{1}{\rho_f} \rho_s \rho_w S_s S_w (h_s - h_w) \left(\frac{\underset{\approx}{k} k_{rs}}{S_s \mu_s} - \frac{\underset{\approx}{k} k_{rw}}{S_w \mu_w} \right)$$

Note that at the boundary between the water and two–phase regions the nonlinear coefficients are actually multi–valued, some with a range of several orders of magnitude. Similar relationships are observed for the other nonlinear coefficients on Eqns. (1) and (2). When these coefficients are not handled carefully, instability, oscillations, and non–convergence in the numerical solution result in the neighborhood of the two–phase boundary.

Let us now examine this phenomenon in detail, using the hypothetical step-function coefficient $C(H)$ illustrated in Fig. 2. The behavior of C as a function of the thermodynamic variable H exhibits two undesirable traits: (a) the step does not propagate accurately as a function of H; (b) the value of C is hypersensitive to the value of H. If we assume a simple analytical relationship for H, i.e., $H(x,t) = (ax+b)(ct+d)$, we would observe the propagation of $C(x,t)$ illustrated in Fig. 3(a). However, when this continuous solution is replaced by a finite element approximation, such as illustrated in Fig. 3(b), the nonlinear coefficient is propagated as shown in Fig. 3(c). The numerical scheme clearly introduces a serious error in the propagation of this coefficient.

4.0 The Inverse Iteration Method

This numerical difficulty can be overcome if one employs a weighted-average value of C(H). We will define C(H) at any node i by

$$C(H) = \sigma(C^{+} - C^{-}) + C^{-} \quad , \qquad 0 \leq \sigma \leq 1$$

when the step lies within the region of influence of node i. We will address the problem of computing σ later. A judicious choice of σ generates the step function propagation illustrated in Fig. 4. Notice that now the step travels with a velocity almost exactly equal to the original smooth velocity shown in Fig. 3(a).

To demonstrate the hypersensitivity of C(H), a one-dimensional experiment was conducted. A phase change from water to steam takes place at some point in the domain. Because no constraints were imposed on the system, the solution exhibited instability and oscillations at nodes near the region where the step change in coefficients occurred. It was observed that on some time steps the node nearest the step change in C(H), node k_*, oscillated exactly between solutions located on either side of the step ($H_* + \varepsilon$ and $H_* - \varepsilon$ of Fig. 2). The associated coefficient oscillation was between C^{+} and C^{-}. When the coefficient was held arbitrarily to C^{+}, a stable non-oscillatory solution was obtained for node k. The solution, however, was $H_* - \varepsilon$, which is compatible with the coefficient C^{-}. When C(H) was arbitrarily held at C^{-}, a solution $H_* = \varepsilon$ was obtained; this is compatible with the coefficient C^{+}. This perfect oscillation suggests that $H_* + \varepsilon$ and $H_* - \varepsilon$ do not represent the correct solution, and that C^{+} and C^{-} are not the appropriate coefficients. The correct solution at node k must be exactly at the coefficient step, i.e., H_* and the correct coefficient value must lie between C^{+} and C^{-}. This hypothesis was tested by trying different values of σ, $0 \leq \sigma \leq 1$, to determine whether there was one value which would yield a solution $H|_k = H_*$. Such a value was indeed obtained, and demonstrated that it was possible to have a set of C(H) and H which was self-consistent in the sense that they both were located at the step function change. Thus it is possible to perform an iterative search for a suitable σ using solution consistency as a constraint (see Fig. 5).

5.0 Summary

Whenever one encounters a geothermal reservoir problem wherein the geothermal fluid flashes from water to steam, the governing equations become highly nonlinear. Oscillatory and non-convergent solutions are sometimes encountered for selected nodes and time steps. The correct solution may reside exactly on the two-phase boundary and require coefficient values which are neither those of the single-phase region nor the two-phase region, but rather a weighted average of the two. An inverse iterative scheme based on the requirement of self-consistency in the solution has been developed to identify the value of the optimal weighting coefficient.

6.0 Notation

6.1 Letters

	Nonlinear coefficient.
g	Gravitational acceleration.
h	Enthalpy.
H	Thermodynamic property used as independent variable.
k	Permeability.
k_r	Relative permeability.
P	Hydrodynamic pressure.
S	Saturation.
T	Temperature.
V	Velocity.
Ax_x	Spatial increment.
E	Small increment.
κ	Thermal conductivity.
e	Porosity.
ρ	Density.
σ	Weighting factor for nonlinear coefficients.
μ	Viscosity

6.2 Subscripts

f	Reservoir fluid
i,k	Nodal numbers.
m	Solid grains.
s	Steam phase.
w	Water phase.

7.0 References Cited

Voss, C. I., Finite Element Simulation of Multiphase Geothermal Reservoirs. Ph.D. Thesis, Princeton University, 1978.

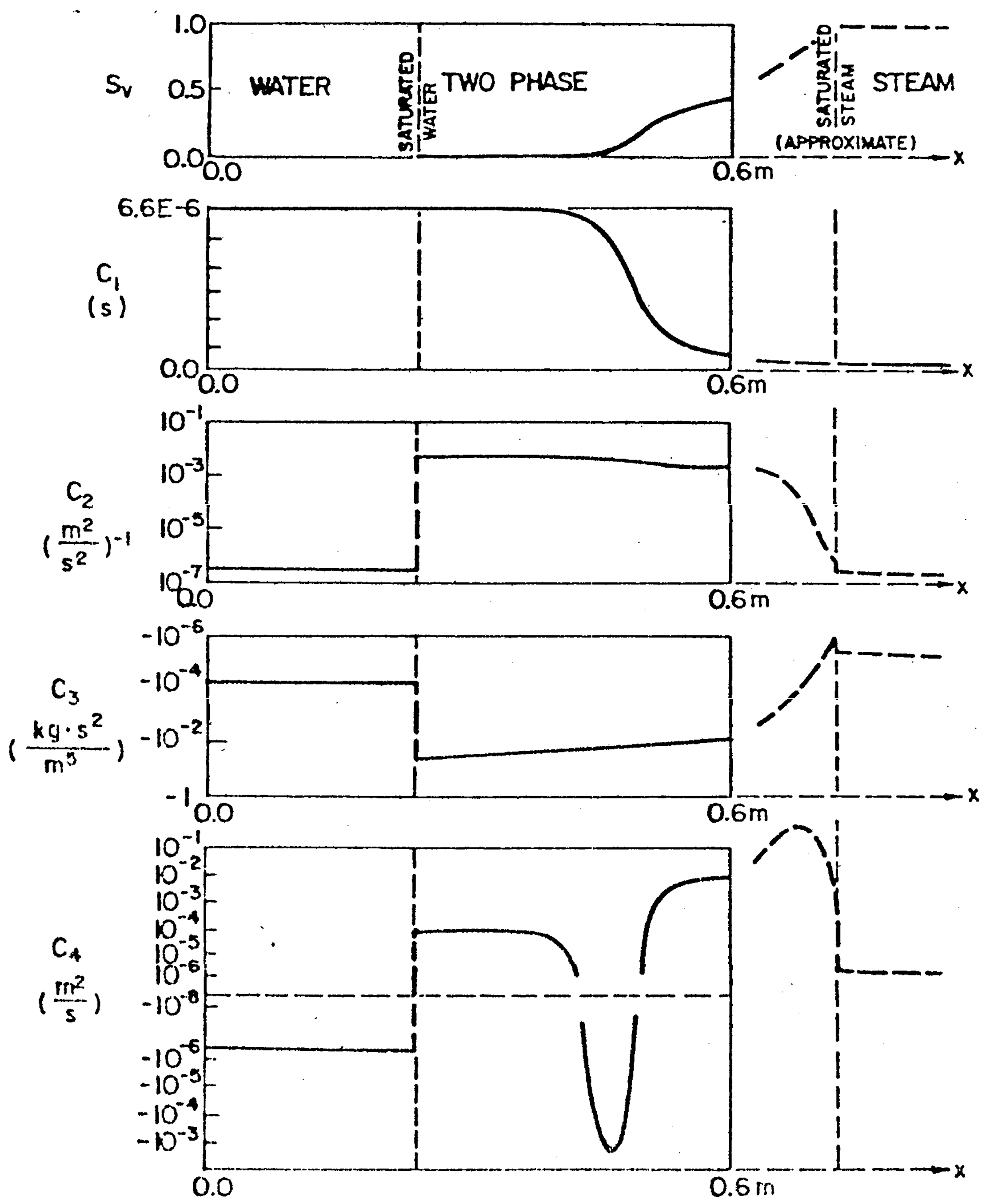

Fig. 1. Nonlinear coefficients for two-phase, non-isothermal problem (after Voss, 1978).

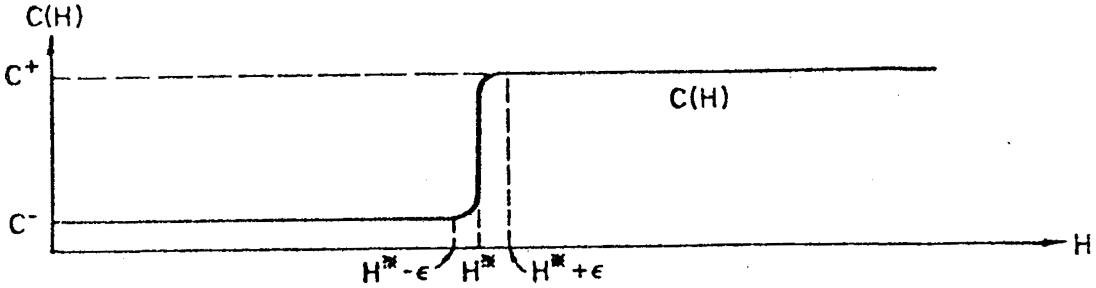

Fig. 2. Hypothetical step-function coefficient C(H) (after Voss, 1978).

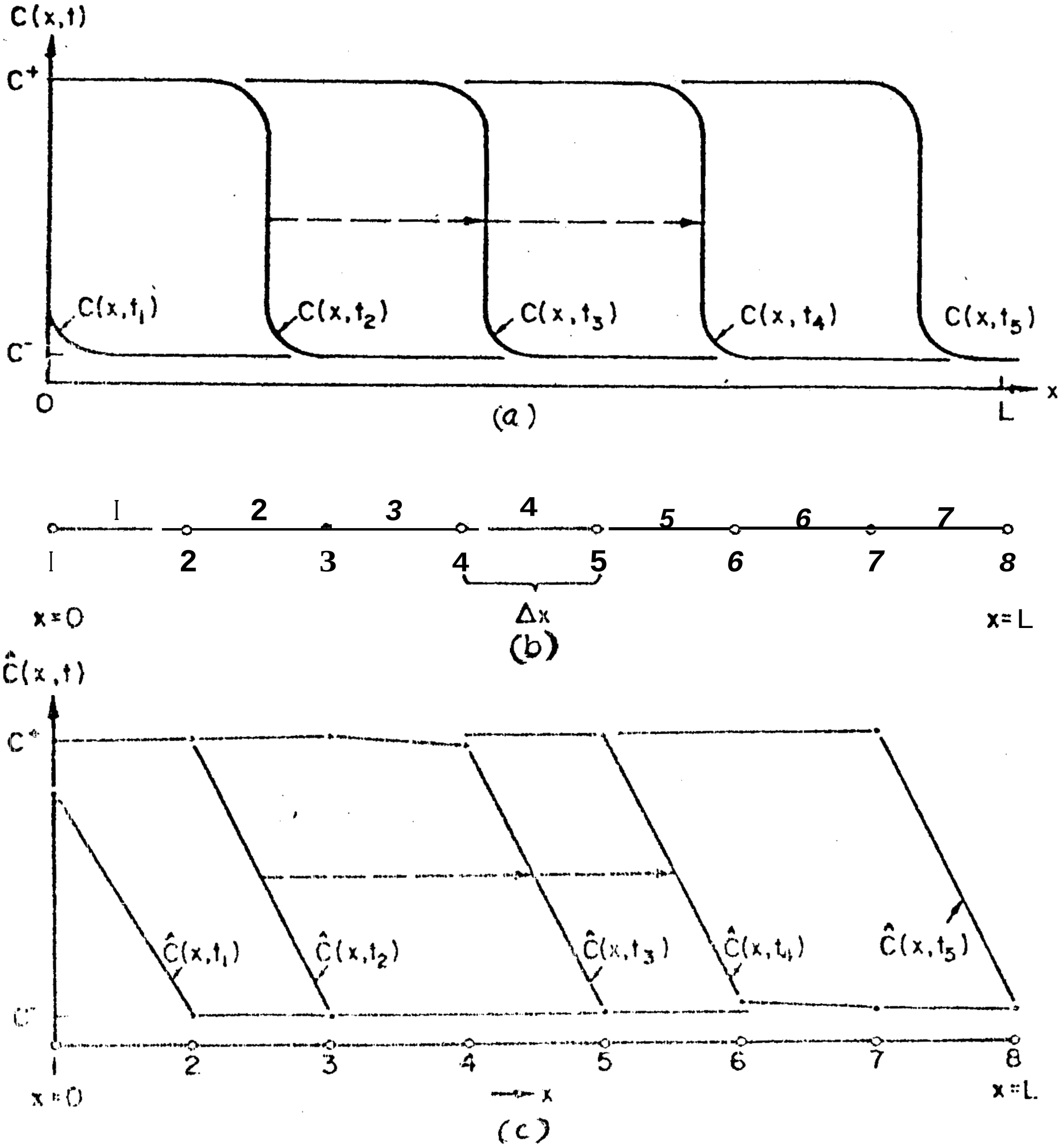

Fig. 3. (a) Smooth progression of nonlinear coefficient, (b) finite element net in one dimension, (c) progression of nonlinear coefficient with discretized operator (after Voss, 1978).

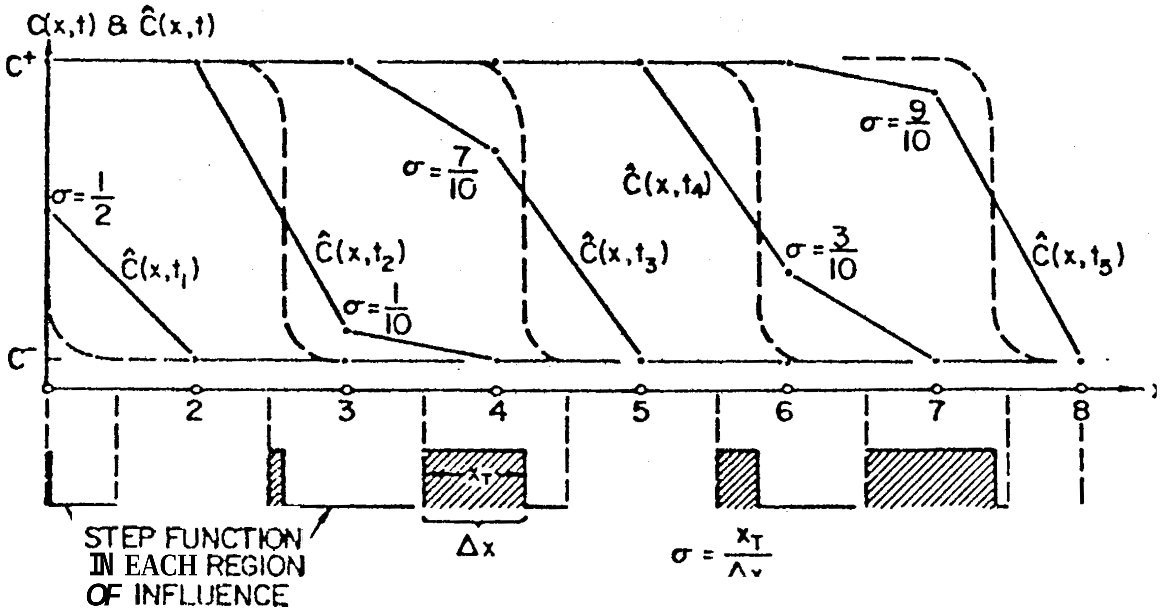

Fig. 4. Propagation of nonlinear coefficient using correction procedure (after Voss, 1978).

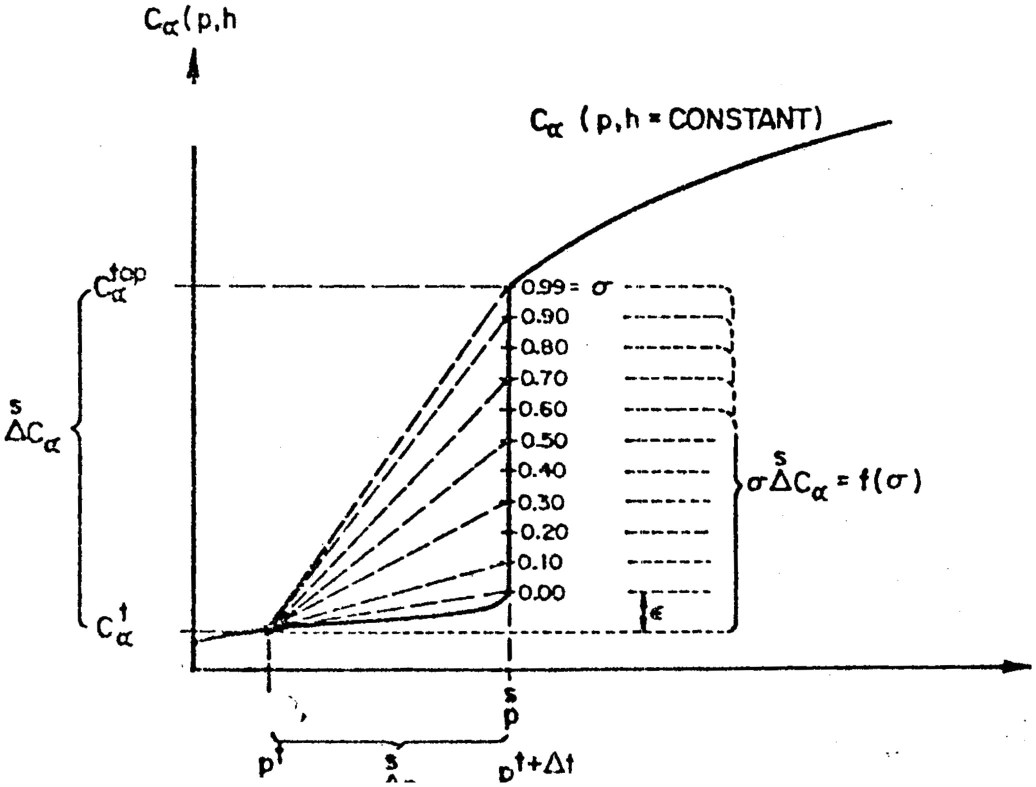

NOTE THAT ε HAS BEEN EXAGGERATED AND IS ACTUALLY VERY SMALL

Fig. 5. Inverse iteration algorithm (after Voss, 1978).